Large Lattice Discretization Effects on the Phase Coexistence of Ionic Fluids

Athanassios Z. Panagiotopoulos*
Institute for Physical Science and Technology and Department of Chemical Engineering, University of Maryland, College Park, Maryland 20742-2431

Sanat K. Kumar†
Department of Materials Science and Engineering, Pennsylvania State University, University Park, Pennsylvania 16802
(Received 14 June 1999)

We examine the phase behavior of lattice restricted primitive models for integer values of the ratio of ionic diameter to lattice spacing, ξ. For $\xi \leq 2$, there is coexistence between a disordered phase and an antiferromagnetic phase, but no vapor-liquid equilibrium. For $\xi \geq 3$, a region of normal vapor-liquid coexistence is found, with critical temperatures and densities which are very close to their continuous space counterparts. Our findings stress that lattice structure can result in qualitatively different physics from continuous space models, but that the two models converge even for relatively coarsely discretized lattices.

PACS numbers: 64.70.Fx, 05.70.Fh, 64.60.Kw

The liquid-vapor coexistence of the restricted primitive model (RPM), which in its simplest form corresponds to an equal number of oppositely charged hard spheres, has been the subject of numerous theoretical [1–5] and simulation [6–12] studies. While there is reasonable agreement between the two most recent simulation studies [11,12], there has been considerable variability in the estimated critical parameters of this model. These inaccuracies can be directly attributed to computational and sampling difficulties associated with simulations of this model. Additional difficulties arise when one considers the lattice analog of the RPM, where each charged site occupies exactly one lattice site [13]. Dickman and Stell [14] have found that there is a first-order transition between a disordered and an antiferromagnetically ordered phase at temperatures below a tricritical point, T_c. Above T_c, there is a line of second-order transitions between a disordered and an antiferromagnetic phase. Clearly, the behavior of the lattice model is qualitatively different from its continuous space analog. There is a tricritical (rather than critical) point, and there is no vapor-liquid transition.

To understand and resolve this discrepancy, we have focused on a class of lattice-based restricted primitive models for which the ratio of ion size to the lattice unit cell dimension, ξ, is varied systematically. We find that, for $\xi \leq 2$, the models yield coexistence between a disordered and an antiferromagnetic phase as found previously by Dickman and Stell [14]. For larger, integer values of ξ, a regular vapor-liquid coexistence occurs with critical temperatures and densities approaching the continuous limit with increasing ξ. For $\xi \geq 4$, we find that the critical temperatures are within 5% of their continuous space analogs, while the critical densities are virtually identical. These facts are particularly important since we can use the advantages of a lattice model, i.e., larger simulation volumes and shorter computational times, to reproduce the continuous limit which has been difficult to simulate accurately.

The lattice RPM model consists of an equal number $N_\pm$ of positive and negative ions of diameter σ on a simple cubic lattice of volume V. The key idea in this work is to start from the $\xi = 1$ model and systematically refine the spacing lattice so that the model can approach the continuous-space analog to an arbitrary degree. The models studied are schematically illustrated in Fig. 1. A two-dimensional projection is used for simplicity in Fig. 1, even though all our calculations were for three-dimensional systems. For $\xi = 1$, a single lattice site is excluded by each ion. For $\xi = 2$, the total number of excluded sites is 27 (a cube of size $3 \times 3 \times 3$) while for higher ξ the shape of the excluded volume of each ion takes on an increasingly spherical shape. The number of excluded sites is 93, 251, and 485, respectively, for $\xi = 3$, 4, and 5. The reduced density ρ^* is defined as $\rho^* = 2N_\pm\sigma^3/V$. Since we describe the volume in units

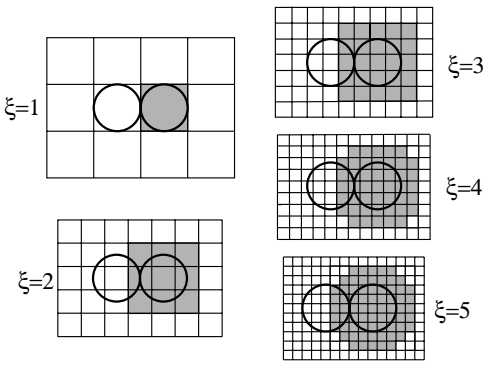

FIG. 1. Projection in two dimensions of the three-dimensional models studied. Two ions at contact are represented for each case. The shaded cells fall within the excluded volume of the ion at right.

of σ^3, the quantity ξ is not utilized in the description of ρ^*. Consequently, $\rho^* = 1$ always corresponds to a fully filled lattice, independent of ξ. A reduced volume of $V^* = V/\sigma^3 = 12^3$ was used for all phase diagram calculations, except near the critical points, for which volumes of 15^3, 19^3, and 24^3 were also used.

Coulombic interactions between ions are given by $U(r) = \pm 1/r$, for like and unlike ions, respectively, where r is the distance, in units of σ, between the centers of the lattice sites occupied by each ion. An important point here is that, since the Coulomb interactions are long ranged, the potential calculations have to include interactions with particles in all images of the periodic box utilized in the calculations. A method to achieve this in the case of electrostatic interactions is the Ewald sum, which is described in detail in standard textbooks, e.g., [15]. An extremely fast table lookup algorithm equivalent to an Ewald sum with a large number of Fourier-space wave vectors was developed to compute the infinite-range ionic interactions. The algorithm is analogous to that used in [16] for investigating lattice systems with long-range interactions. It involves precomputing the Coulomb interaction between any two sites on the lattice, including all periodic images of the sites to an infinite distance. The summation is performed with the standard Ewald sum with vacuum boundary conditions, 518 Fourier-space wave vectors and real-space damping parameter $\kappa = 5$. The Ewald sum is performed only *once*, at the beginning of the simulation, and the translationally invariant contributions stored in an array. The relative acceleration for the lattice calculations versus our earlier off-lattice calculations for the RPM was a factor of at least 100.

We determined the phase coexistence of these solutions by the histogram reweighting method [17,18]. For a system of volume V in the grand canonical ensemble the probability of its occurrence with energy E and number of particles N_p, $f(N_p, E)$, is

$$f(N_p, E) \equiv \frac{\Omega(N_p, V, E) \exp[-\beta E + \beta \mu N_p]}{\Xi(\mu, V, T)} . \quad (1)$$

$\beta \equiv 1/k_B T$, μ is the chemical potential, and $\Xi(\mu, V, T)$ is the grand partition function. $\Omega(N_p, V, E)$ is the microcanonical partition function. One performs a series of grand canonical Monte Carlo simulations with a fixed value of T and μ in each one. Only ion pair additions and removals were attempted, and, hence, μ corresponds to this elementary, charge neutral pair. To enhance acceptance of the insertion and removal steps for these strongly interacting Coulombic systems, a distance-biasing algorithm [10] was used. We used the Boltzmann factor of the interaction energy of a pair at a given separation as the distance-biasing factor. Combining the simulations yields an estimate of $\Omega(N_p, V, E)$ to within an arbitrary constant, from which system thermodynamics are derived.

Our results for the first-order transition curves for the $\xi = 1$ and $\xi = 2$ cases are shown in Fig. 2 as open circles and triangles, respectively. In both cases, coexistence is between a low-density disordered phase and an antiferromagnetically ordered high-density phase. The $\xi = 1$ results are quite similar to those of Dickman and Stell [14], with the exception that our calculations extend nearer to the tricritical point, for which our estimate is $T_c^* = 0.15 \pm 0.01$, $\rho_c^* = 0.48 \pm 0.02$. This estimate is based on a linear extrapolation of the coexistence line, as expected for $d = 3$ tricriticality. Our estimate is probably an upper bound to the true tricritical temperature, since it is based on small system size simulations. The presence of a tricritical point in the $\xi = 1$ model has been predicted from the theoretical analysis of Høye and Stell [19]. The filled circles and dashed line indicate a preliminary estimate of the Néel line of continuous transitions from disordered to antiferromagnetic structures, obtained by locating a peak in the constant-volume heat capacity at three temperatures. The line is nearly vertical, while in the results of Dickman and Stell the line has a lower slope, at least for $T^* \geq 0.2$. Detailed finite-size scaling analysis will be required for resolution of the exact location of the line of second-order transitions.

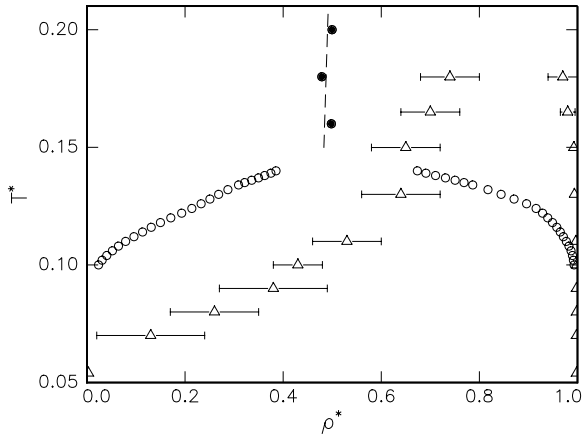

FIG. 2. Phase behavior of the $\xi = 1$ and $\xi = 2$ models. Open circles are for the first-order transition for $\xi = 1$; filled circles and dashed line are for the Néel line for $\xi = 1$. Open triangles are for the first-order transition for $\xi = 2$, with large uncertainties due to the presence of hysteresis loops.

The $\xi = 2$ model presented special difficulties. There was a range of chemical potentials over which hysteresis loops were observed. Over that range, a run initiated at low density would remain in an apparently stable disordered low-density state even after 2×10^8 Monte Carlo pair addition and removal steps. On increase of the chemical potential outside the hysteresis region, it would slowly convert to a nearly perfect antiferromagnetic high-density state. Conversely, a run started from a high-density ordered state would remain stable over a range of chemical potentials overlapping with the range of stability of the low-density state. Hysteresis loops are expected whenever first-order transitions are present. However, for the other cases studied in this paper, we were able

to obtain the equilibrium coexistence curves with low uncertainties by linking states on opposite sides of the coexistence curve through simulations above a critical (or tricritical in the case $\xi = 1$) point. In the case $\xi = 2$, the critical or tricritical point occurs at very high densities, $\rho^* \geq 0.8$. We were unable to obtain adequately sampled states at these very high densities for constructing an equilibrium free-energy surface. The first-order transition density, however, is by necessity bounded from above and below by the densities at the extremes of the hysteresis loop. The midpoint density of the hysteresis loop is shown in Fig. 2 as the low-density coexistence point, with (large) error bars covering the range of hysteresis.

The two coexisting phases for the $\xi = 2$ model are qualitatively similar to the disordered and antiferromagnetically ordered states for $\xi = 1$, except for a shift of the transition to higher densities. We suggest the following physical reason for this shift. For the $\xi = 2$ model, displacement of an ordered structure by a single lattice spacing along any of the principal directions results in a new structure *incommensurate* with the previous one. This is not the case for the $\xi = 1$ model, for which displacement by one lattice spacing does not change the overall structure, except for interchange of positive and negative ions.

Our results for $\xi = 3$, 4, and 5 are shown in Fig. 3, together with previous calculations for the continuous-space RPM [12]. Critical points for the lattice RPM models were estimated using mixed-field finite-size scaling methods [20], assuming that the systems belong to the Ising universality class. In all cases, our results for the critical distribution and for the system-size dependence of the critical parameters were highly consistent with the hypothesis of Ising criticality. The use of larger system sizes than in previous continuous-space studies provides a more stringent test of this assumption. Extrapolated critical points for infinite system size and subcritical vapor-liquid coexistence curves are shown on Fig. 3. Clearly,

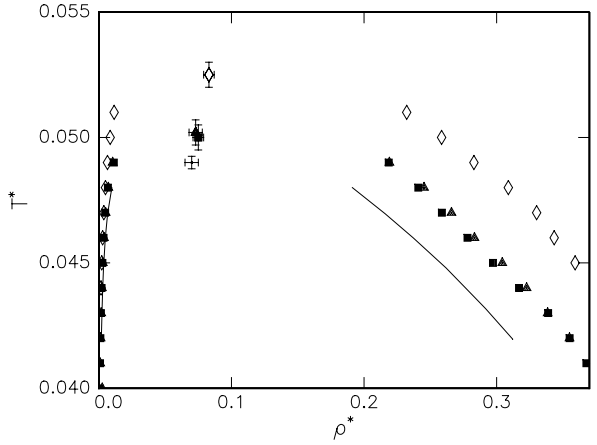

FIG. 3. Phase behavior of the $\xi = 3$, 4, and 5 models (diamonds, filled squares, and filled triangles, respectively) and the continuous-space RPM (line).

the behavior of the lattice RPM models for the finely discretized lattices is quite similar to the continuous-space RPM. Already at $\xi = 4$, the difference in the critical temperature is less than 5% and the critical density is higher by an amount less than the combined simulation uncertainties.

The solid-liquid coexistence of the continuous-space restricted primitive model has been studied by Smit *et al.* [21]. Liquid-solid phase coexistence was observed above the triple point located at approximately $T^* = 0.025$. The solid phase that first forms from the liquid at low temperatures has a body-centered-cubic structure. Using these results for guidance, we expect that the $\xi \geq 3$ models will exhibit transitions to an ordered phase over the temperature range of Fig. 2 at sufficiently high densities. These liquid-solid transitions can be considered a natural continuation of the order-disorder transitions observed for $\xi = 1$ and 2, now shifted to even lower temperatures. In essence, the absence of liquid-vapor transitions for the $\xi = 1$ and 2 cases is simply a manifestation of the tendency of the low-ξ models to solidify before forming a "proper" liquid. This situation has been seen previously in off-lattice models with extremely short-range interactions [22] and lattice models with weak long-range interactions [23], but not, to the best of our knowledge, in systems with strong long-range interactions. Dipolar hard sphere and spherocylinder systems also do not have a liquid phase [24], but the reason for the absence of a liquid is the formation of chains in the low-density gas, rather than solidification.

The possible presence of both a normal critical and a tricritical point in RPM-type models has been anticipated on theoretical grounds by Ciach and Stell [25]. Our numerical calculations provide support for this suggestion for $\xi \geq 3$. Since the densities at which this transition will occur are likely to be greater than for $\xi = 2$, for which we already encountered sampling difficulties, a complete numerical confirmation of this suggestion will have to be based on more efficient sampling methods than the ones used in this work.

In summary, we have computed the phase diagrams of a series of related lattice restricted primitive models. For the coarsely discretized models, order-disorder transitions occur at sufficiently high temperatures to preempt the normal vapor-liquid critical point. The phase behavior of finely discretized models approaches that of the continuous-space analog quite rapidly. However, even finely discretized lattice models retain a large computational advantage over their continuous-space counterparts. This opens up the possibility of detailed studies by simulation of the phase and aggregation behavior of ionic solutions beyond the restricted primitive model.

Funding for this research was provided by the Department of Energy [DE-FG02-98ER14858, A. Z. P.] and the National Science Foundation [CTS-9704907, S. K. K.]. We thank Michael Fisher and Gerassimos Orkoulas for

helpful discussions and comments on the manuscript and George Stell for extensive correspondence and for providing reprints and copies of manuscripts prior to publication.

*To whom correspondence should be addressed.
Electronic address: thanos@ipst.umd.edu
†Electronic address: kumar@plmsc.psu.edu

[1] G. Stell, K. C. Wu, and B. Larsen, Phys. Rev. Lett. **37**, 1369 (1976); Y. Zhou, S. Yeh, and G. Stell, J. Chem. Phys. **102**, 5785 (1995).
[2] M. Rovere, R. Miniero, M. Parrinelo, and M. P. Tosi, Phys. Chem. Liq. **9**, 11 (1979).
[3] H. L. Friedman and B. J. Larsen, J. Chem. Phys. **70**, 92 (1979).
[4] W. Ebeling and M. Grigo, Ann. Phys. (Leipzig) **37**, 21 (1980).
[5] M. E. Fisher and Y. Levin, Phys. Rev. Lett. **71**, 3826 (1993); B. J. Lee and M. E. Fisher, Phys. Rev. Lett. **76**, 2906 (1996); D. M. Zuckerman, M. E. Fisher, and B. P. Lee, Phys. Rev. E **56**, 6569 (1997).
[6] P. N. Vorontsov-Velyaminov and V. P. Chasovskikh, High Temp. (USSR) **13**, 1071 (1975).
[7] M. J. Gillan, Mol. Phys. **49**, 421 (1983).
[8] K. S. Pitzer and D. R. Schreiber, Mol. Phys. **60**, 1067 (1987).
[9] J. P. Valleau, J. Chem. Phys. **95**, 584 (1991).
[10] G. Orkoulas and A. Z. Panagiotopoulos, J. Chem. Phys. **101**, 1452 (1994).
[11] J. M. Caillol, D. Levesque, and J. J. Weis, Phys. Rev. Lett. **77**, 4039 (1996); J. Chem. Phys. **107**, 1565 (1997).
[12] G. Orkoulas and A. Z. Panagiotopoulos, J. Chem. Phys. **110**, 1581 (1999).
[13] A. B. Walker and M. J. Gillan, J. Phys. C, Solid State Phys. **16**, 3025 (1983).
[14] G. Stell, in *New Approaches to Problems in Liquid State Theory*, edited by C. Caccamo, J.-P. Hansen, and G. Stell, NATO ASI, Ser. C (Kluwer, Dordrecht, 1999), pp. 71–89. Figure 2 of this reference provides Monte Carlo results of Dickman and Stell for the $\xi = 1$ model studied here.
[15] M. P. Allan and D. J. Tildesley, *Computer Simulations of Liquids* (Oxford University, New York, 1987).
[16] E. Luijten and K. Binder, Phys. Rev. E **58**, R4060 (1998).
[17] A. M. Ferrenberg and R. H. Swendsen, Phys. Rev. Lett. **61**, 2635 (1988).
[18] A. M. Ferrenberg and R. H. Swendsen, Phys. Rev. Lett. **63**, 1195 (1989).
[19] J. S. Høye and G. Stell, J. Stat. Phys. **89**, 177 (1997).
[20] A. D. Bruce and N. B. Wilding, Phys. Rev. Lett. **68**, 193 (1992); N. B. Wilding and A. D. Bruce, J. Phys. Condens. Matter **4**, 3087 (1992).
[21] B. Smit, K. Esselink, and D. Frenkel, Mol. Phys. **87**, 159 (1996).
[22] P. R. ten Wolde and D. Frenkel, Science **277**, 1975 (1997).
[23] G. Stell, H. Narang, and C. K. Hall, Phys. Rev. Lett. **28**, 292 (1972); C. K. Hall and G. Stell, Phys. Rev. A **7**, 1679 (1973).
[24] M. E. Van Leeuwen and B. Smit, Phys. Rev. Lett. **71**, 3991 (1993); S. C. McGrother and G. Jackson, Phys. Rev. Lett. **76**, 4183 (1996).
[25] A. Ciach and G. Stell, J. Mol. Fluids (to be published).